The Relationship of Agarose Gel Structure to the Sieving of Spheres during Agarose Gel Electrophoresis

Gary A. Griess,* Kenneth B. Guiseley,‡ and Philip Serwer*‡
*Department of Biochemistry, The University of Texas Health Science Center, San Antonio, Texas 78284-7760 and ‡FMC Bioproducts, Rockland, Maine 04841 USA

ABSTRACT To understand the organization of fibers in an agarose gel, digitized electron micrographs are used here to determine the frequency distribution of interfiber distance ($2P_c$) in thin sections of agarose gels. For a preparation of underivatized agarose, a 1.5% gel has a P_c distribution that is indistinguishable from the P_c distribution of a computer-generated, random-fiber gel; the log of the occurrence frequency (F) decreases linearly as a function of P_c. As the agarose concentration decreases below 1.5%, the semilogarithmic F versus P_c plot becomes progressively less linear. Two straight lines represent the data; the plot is steeper at the lower P_c values. As the percentage of agarose increases above 1.5%, the semilogarithmic F versus P_c plot becomes steeper at the higher P_c values. This change in the shape of semilogarithmic F versus P_c plots is possibly explained by the existence in agarose gels of two zones, one whose P_c distribution is more sensitive to the average agarose concentration than the other. To compare the structure of agarose gels to their sieving during electrophoresis, the root mean square value of P_c ($\hat{P}_c$) is compared to the sieving-based radius of the effective pore (P_E; Griess *et al.* (16)) for both underivatized agarose and a derivatized agarose that has a smaller P_E at any given agarose percentage. For 0.8–2.0% gels of either underivatized or derivatized agarose, $P_E/\hat{P}_c$ is a constant within experimental error. Deviations from this constant are observed at lower gel percentages. This relationship of P_E to $\hat{P}_c$ constrains theoretical descriptions of the motion of spheres in fibrous networks.

INTRODUCTION

Gel electrophoresis is used to fractionate particles as small as a nucleotide (size, about 2 nm; reviewed in Ref. 1) and as large as a bacterial cell (size, 1000–3000 nm; reviewed in Ref. 2). Random coils, such as double-stranded DNA molecules, are also among the particles fractionated. Although electrophoretic fractionation of DNA can be treated empirically (for example: Ref. 1), the conformation of DNA longer than 20–40 kilobases pairs (kb)[1] exhibits gel electrophoresis-induced hysteresis that, for the following reasons, has stimulated interest in the mechanisms by which DNA is retarded by the hydrodynamic and steric effects of the gel (to be collectively called sieving): (*a*) By periodically varying either the direction or the intensity of the electrical field during agarose gel electrophoresis (pulsed field gel electrophoresis, or PFGE), the conformational hysteresis of DNA can be used to improve fractionation of both linear double-stranded DNA as long as 6,000 kilobase pairs (kb) and open circular DNA as long as 300 kb (reviewed in Refs. 2–6). (*b*) Conformational hysteresis of both DNA and other biological polymers is a possible source of short-term biological memory. For the various models constructed to correlate macroscopic phenomena with microscopic phenomena for both PFGE and the constant field gel electrophoresis of DNA, the distribution of fibers in a gel has been a subject of conjecture. Empirical determination of this distribution was not made (5–8). Even for modeling the migration of solid spheres in agarose gels, no dynamic model has been developed and tested by use of empirical structural information about the gel. For example, no correlation of the macroscopically observed sieving of spheres has been made with the dimensions of spaces observed in the network of gel used to obtain sieving.

During attempts to empirically determine the distribution of fibers in agarose gels, electron microscopy of thin sections has revealed 4% agarose beads to be networks of fibers; each fiber consists of laterally aggregated narrower strands of an agarose polysaccharide chain (9, 10). This observation has been confirmed by use of specimens prepared by freeze-etching (11, 12). The lateral aggregation has also been observed during both studies of agarose in solution (13, 14) and electron microscopy of negatively stained agarose fibers broken from the network of gel (2). For performing a statistical analysis of interfiber distances, electron micrographs of thin sections appear to have the appropriate information. However, with the exception of a preliminary study (15), thin sections of agarose gels used for electrophoresis have not been obtained; statistical analysis of interfiber distances has not been made.

By use of theory based on either hydrodynamics or sterics, the electrophoretic sieving of spheres in agarose gels is quantitatively described by use of one agarose gel-based characteristic: the radius of the effective pore, P_E (16). Thus, in

Received for publication 22 January 1993 and in final form 3 March 1993.
Address reprint requests to Philip Serwer. Tel.: 210-567-3765; Fax: 210-567-6595.

[1] *Abbreviations used*: kb, kilobase pairs; PFGE, pulsed field agarose gel electrophoresis; P_E, radius of the effective pore of a gel; A, percentage of agarose in a gel; P_c, one-half the length of a line segment (chord) between two nearest neighboring fibers in a two-dimensional projection of a gel; F, the fraction of chords that have a length of $2P_c$; L_V, total length of agarose fibers per nm^3; M_L, mean mass of agarose fiber per nanometer; k_1, k_2, slopes of a semilogarithmic F versus P_c plot, at the lower and higher P_c values, respectively; $\bar{P}_c$, mean value of P_c; $\hat{P}_c$, root mean square value of P_c; x, slope of a log-log plot of either an averaged P_c or P_E versus A; σ, standard deviation of P_c.

0006-3495/93/07/138/11 $2.00

the present communication, values of P_E have been correlated with structural characteristics obtained by statistical analysis of the interfiber distances in electron micrographs of thin sections of 0.4–2.5% agarose gels used for electrophoresis. Implications for understanding both the sieving and structure of agarose gels are discussed.

MATERIALS AND METHODS

Casting of agarose gels

Agarose was dissolved in glass distilled water by boiling in a microwave oven; the weight of water lost during boiling was determined; evaporated water was replaced. After equilibration of the agarose solution at 60–65°C, the following electrophoresis buffer was added from a 10 × concentrated stock solution: 0.025 M sodium phosphate, pH 7.4, 0.001 M $MgCl_2$. Subsequently, agarose gels (running gels) were cast at room temperature (22 ± 3°C) within a precast frame of Seakem LE agarose (FMC Bioproducts, Rockland, ME), by use of framing procedures previously described; the composite gel formed is called a multigel (17). After equilibration overnight at room temperature against electrophoresis buffer, the separate running gels were used for electrophoresis, according to procedures described in the next section. Underivatized agarose used for running gels was Seakem LE agarose (lot 61569; FMC Bioproducts). Derivatized agarose used for running gels was hydroxypropyl agarose, prepared by reacting Seakem Gold agarose (FMC Bioproducts) (18) with propylene oxide, according to procedures previously described (19). At a concentration of 1%, the strength of hydroxypropyl agarose cast in water was 216 g/cm^2. At a concentration of 1.5%, gelling temperature was 27.5°C; melting temperature was 67°C.

Quantification of sieving

Sieving was quantified by measuring the dependence on agarose gel percentage (A) of the electrophoretic mobility of two particles that are 30.1 ± 0.6 nm in radius: bacteriophages T3 and ϕII (20). These bacteriophages had been both prepared by use of procedures previously described (20) and dialyzed against Tris-Mg buffer: 0.2 M NaCl, 0.01 M Tris-Cl, pH 7.4. To prepare T3 and ϕII for electrophoresis, a mixture of these two bacteriophages was added to a 4 × volume of 200 μg/ml bromphenol blue, 5% sucrose that had a 1/50 dilution of 1 mg/ml DNase I (Worthington Biochemical Corp.). Fifty μl of the mixture of T3 and ϕII (0.5–2.0 μg each) was layered at the origin of each running gel in a multigel. Subsequently, the gel was subjected to electrophoresis at 1.6 V/cm, 25°C. During electrophoresis, buffer was circulated (17) and temperature was controlled ±0.3°C by use of either procedures previously reviewed (17) or a thermoelectric system more recently developed (21). After electrophoresis, the position of a band was determined by, first, staining with 1 μg/ml ethidium bromide in electrophoresis buffer and, then, staining overnight with 1 μg/ml ethidium bromide in 0.001 M sodium EDTA, pH 7.4. Expulsion of DNA from bacteriophages occurred during the second staining. This expulsion increased the intensity of staining and, therefore, confirmed that the bands observed were formed by intact bacteriophages (not, for example, by DNA that had been expelled from a bacteriophage capsid before staining). Photographs of ethidium-stained gels were made by use of Kodak Tri-X film and a Tiffen 23A (orange) filter. To measure the distance from the electrophoretic origin of a band, video images of photographs were digitized by use of procedures described below. Measuring tools of the program, NIH IMAGE, version 1.40 (22) were used to determine the distance of the center of a band from the origin of electrophoresis. Values of P_E as a function of A were determined from electrophoretic mobility as a function of A, by use of both the radius of the bacteriophage and procedures, including Eq. 3, described in Ref. 16. In all experiments presented here, the P_E value found by use of bacteriophage T3 did not significantly differ from the P_E value found by use of the equally large bacteriophage ϕII. Because the solid-support free electrophoretic mobility of bacteriophage ϕII is 1.3 × that of bacteriophage T3 (20), this equality indicates that gel concentration-dependence of electroosmosis (if any) did not detectably interfere with measurement of P_E.

Thin sectioning and electron microscopy of agarose gels

An agarose gel cast for electrophoresis was prepared for thin-sectioning by, first, excising pieces of agarose that had the dimensions of a cylinder approximately 0.4 cm long and 0.1 cm in diameter. These pieces were rinsed once with 0.1 M sodium phosphate, pH 7.4, and then treated with 1% osmium tetroxide in Zetterquist's buffer (23) for 1.5 h, at room temperature (22 ± 3°C), with gentle agitation. The agarose pieces were then: (*a*) rinsed with three changes of Zetterquist's buffer, (*b*) dehydrated in a series of increasingly more concentrated ethanol solutions (70, 95, 100%), (*c*) soaked in propylene oxide: two fresh changes of 15 min each, (*d*) infiltrated with a 1:1 mixture of propylene oxide and epoxy resin (23) at room temperature, for 1 h, with agitation; the resin was obtained from Polysciences, Inc., Warrington, PA (Poly/Bed 812 embedding kit; number 08792), (*e*) further infiltrated with 100% Poly/Bed 812 for 1 h, followed by a second portion of 100% Poly/Bed 812 overnight. The next morning, fresh resin was added and the resin was polymerized for 3 days at 75°C. Embedded agarose gels varied in color from light gray to black. The extent of blackening could be increased by increasing the time of dehydration; the time of each dehydration step was between 25 and 60 min. The fiber distribution obtained in the Results for a 1.5% underivatized agarose gel was independent of the extent of blackening.

After embedding of agarose gels, dark gold thin sections (120 ± 15 nm in thickness (24–26)) were cut by use of a Dupont-Sorvall MT 5000 ultramicrotome, fitted with a Diatome diamond knife. The sections were: (*a*) collected on a 200-mesh copper grid, (*b*) stained by the procedure of Estrada *et al.* (27), for 20 s with 7% uranyl acetate, followed by 20 s with Reynolds lead citrate (28). Thin sections were observed in a JEOL 100CX electron microscope. Micrographs of randomly chosen areas were taken at an instrumental magnification of approximately 10,000 ×. To determine more precisely the magnification, micrographs of a diffraction grating were taken at the beginning and end of each series of micrographs of agarose gels.

Digitization and processing of images

Both electron micrographs of sectioned gels and photographs of bands formed during gel electrophoresis were digitized via a video camera, by use of procedures previously described (29). Images were processed by use of the program, NIH IMAGE (22). The digitized images (see Fig. 3) were photographically reproduced by procedures previously described (29). A digitized intermediate was not used for Figs. 1 and 2.

Computer simulation of projection of random fiber gels

To produce a computer-simulated two-dimensional projection of a section of a three-dimensional random fiber gel, the following operations were performed by use of a subroutine (available on request) written for NIH IMAGE: (*a*) A fiber was randomly placed by using a random number generator to produce the three Cartesian coordinates of one end of the fiber. (*b*) The fiber was randomly oriented by choosing the two angular coordinates of the other end by use of a random number generator. (*c*) Sectioning was mimicked by eliminating all parts of the fiber that had a Z coordinate (perpendicular to the eventual plane of projection) outside of the section. (*d*) The projection of the (potentially truncated) fiber in the x-y plane was determined. (*e*) Steps 1–4 were repeated until a desired total length of all projected fibers was achieved (this length is indicated under Results). All fibers had the same length before sectioning. This length was chosen by a procedure described under Results.

RESULTS

Appearance of agarose gels in electron micrographs: dependence on gel concentration

To determine the distribution of interfiber distances in agarose gels, thin sections of agarose gels were observed by use

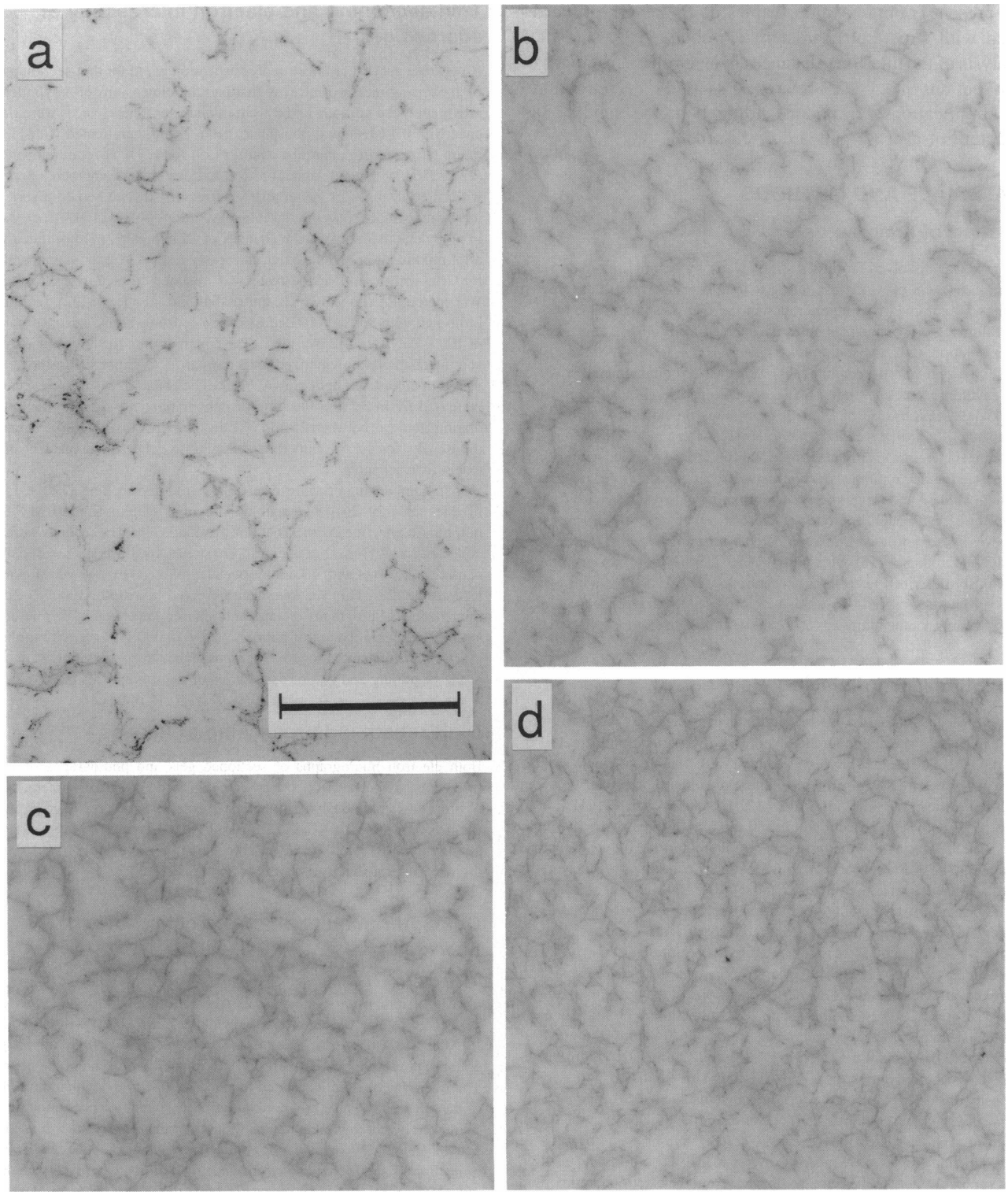

FIGURE 1 Electron micrographs of agarose gels. Electron microscopy was performed by procedures described under Materials and Methods. The *A* value was: 0.4 (*a*), 1.0 (*b*), 1.5 (*c*), 2.5 (*d*). The length of the bar is 2000 nm.

of electron microscopy. This procedure had previously been used to observe agarose fibers in 4% commercial agarose beads (9, 10). In both of these previous studies, no change in macroscopic dimensions of the beads was observed after embedding. Likewise, when pieces of 0.4–2.5% underivatized agarose gels were both excised from running gels used for electrophoresis and embedded by use of the procedure described under Materials and Methods, no change in macroscopic dimensions (±5%) was observed here. Attempts were also made to embed less concentrated gels (0.2%), but these attempts failed because of breakage of the gels.

Qualitatively, electron micrographs revealed agarose fibers in thin sections of the embedded agarose gels. As expected, the apparent total length of fibers increased as the

concentration of agarose increased from 0.4% (Fig. 1 *a*) to 1.0% (Fig. 1 *b*), 1.5% (Fig. 1 *c*), and 2.5% (Fig. 1 *d*); quantification of this increase is in the next section. The observed fibers appeared to both laterally aggregate and branch. The apparent width of these fibers varied from 15 to 30 nm. Thus, as previously found (Introduction), the fibers of Fig. 1 are lateral aggregates of the narrower agarose fibers previously observed by use of both x-ray scattering (30–32) and a negative staining technique of electron microscopy (2). Because the smaller details present are difficult to see in Fig. 1, a more magnified image of a 2.5% agarose gel is shown in Fig. 2. The image of the 0.4% gel in Fig. 1 *a* has fiber-associated comparatively opaque spots of stain that were more numerous than those in the more concentrated gels in Fig. 1, *b–d*. This observation has been reproducibly made for three independently embedded and sectioned gels. As the gel concentration increased in Fig. 1, qualitatively, the gel appeared to become more uniform. However, this type of appearance can be deceptive in the absence of precise quantification. Thus, in the next section, quantification of interfiber spacing is performed.

Quantification of interfiber spacing

To quantify the distribution of interfiber spacing in thin sections of agarose gels, straight lines have been passed through electron micrographs of agarose gels. For each straight line, the length was determined for all line segments (chords) between nearest neighboring contacts with this two-dimensional projection of the network of gel fibers; the length of a chord is called $2P_c$. The coefficient, 2, is used because previous sieving-based quantification of pore dimensions was presented as effective radius, not diameter. To obtain a statistical measure of P_c, electron micrographs of gels were initially converted to binary images that were subsequently analyzed.

The production of a binary image began with digitization of a photographic electron micrograph magnified to 10 nm/pixel (Fig. 3 *a*). Subsequently, noise in the image was reduced by use of a 3×3 median filter (33). To sharpen edges, a 7-pixel by 7-pixel Laplacian filter kernel was convolved with the image. This procedure sharpens edges (34, 35), while (*a*) causing opposing edges of a fiber to merge, thereby preventing the formation of spurious empty spaces, and (*b*) not causing fibers to change in their apparent width (Fig. 3 *b*). After sharpening edges, both thresholding and binarization operations (33, 36) were applied (Fig. 3 *c*). Thresholding eliminates background caused by amplification of residual noise, some of which is produced during digitization. The threshold was adjusted to produce a level of one to two pixel spots that was approximately equal to the level of comparably sized spots on the original electron micrograph (10). To quantify both the total length of agarose fibers per volume (L_V) and the mean mass of agarose per unit length (M_L), fibers in a binarized image of a gel network were converted

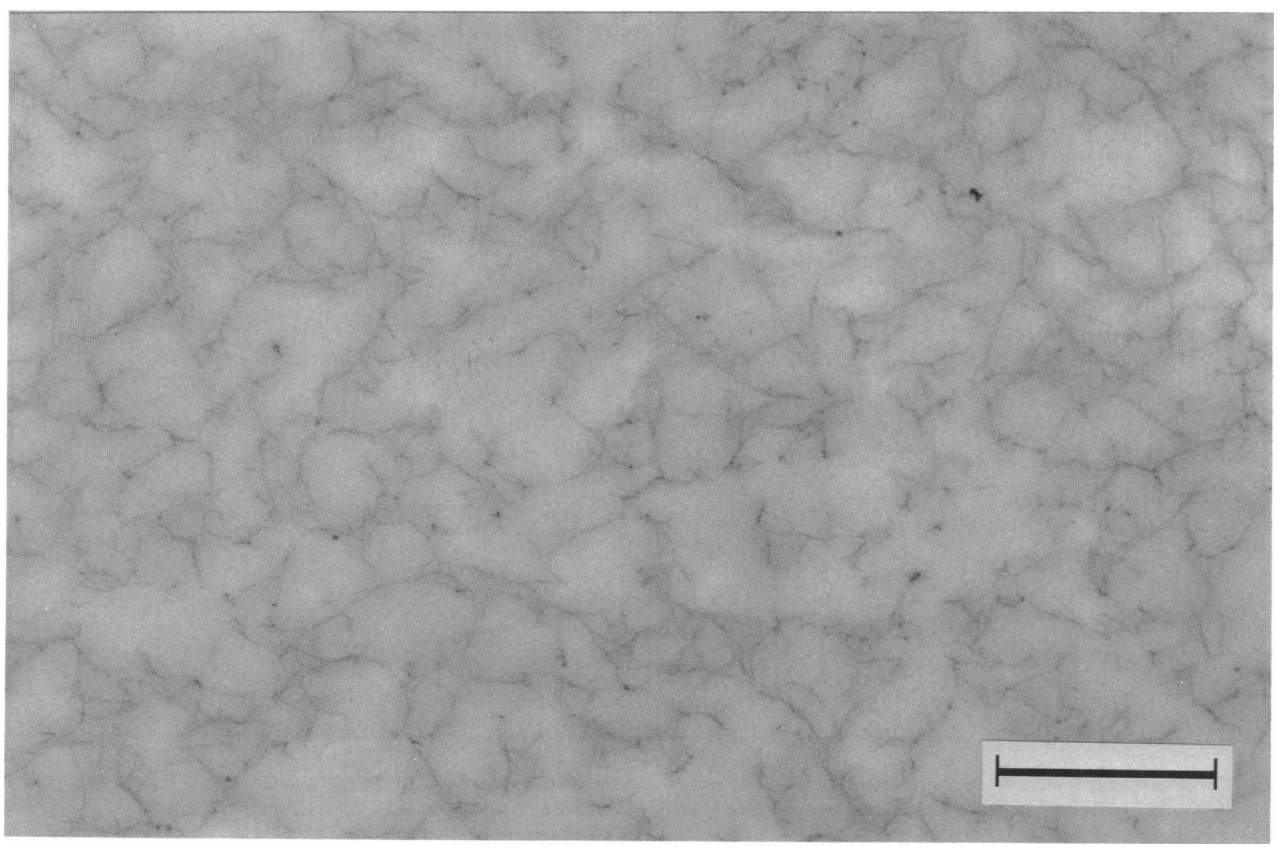

FIGURE 2 Electron microscopy at higher magnification. Electron microscopy of a 2.5% underivatized agarose gel was performed by procedures described under Materials and Methods. The length of the bar is 1000 nm.

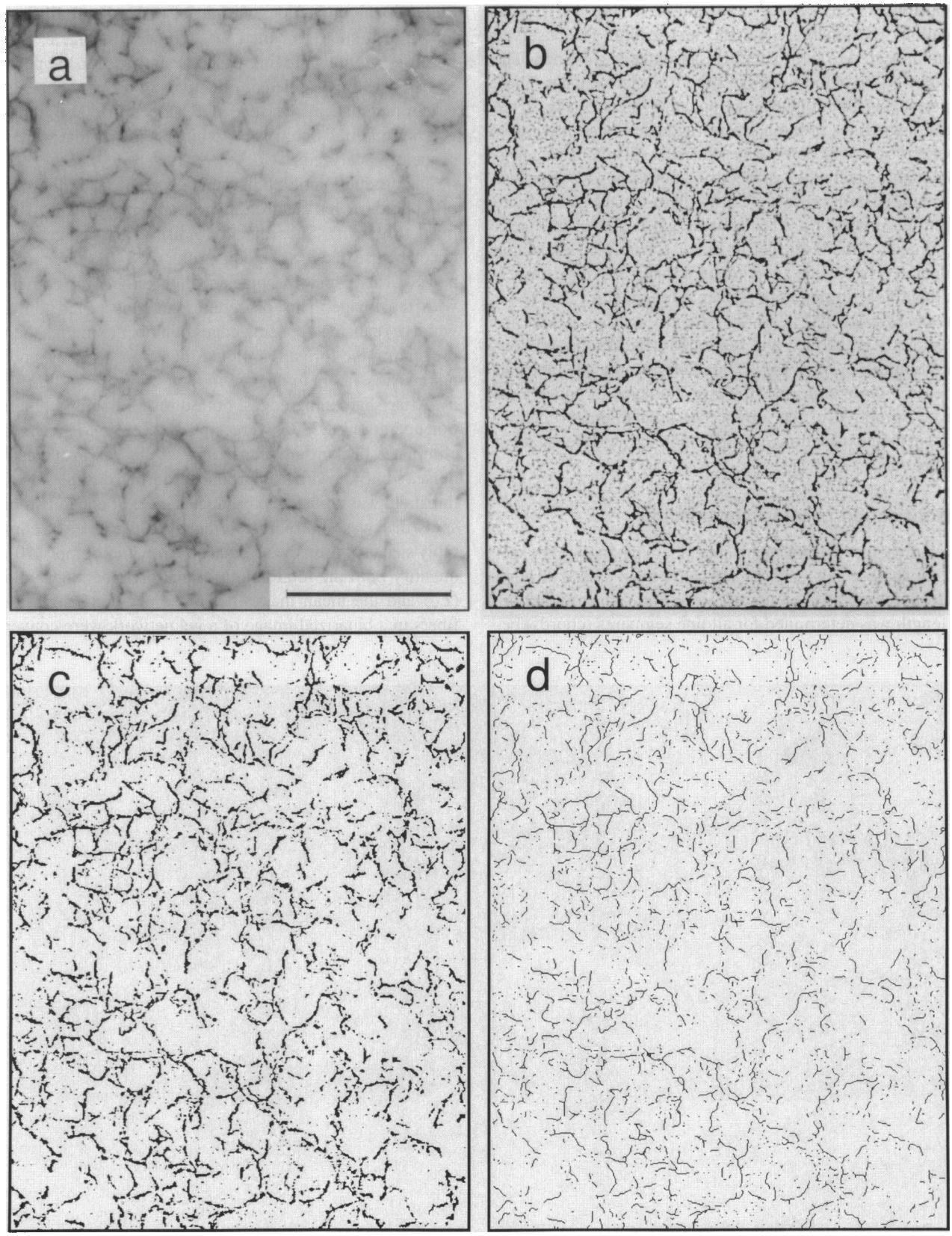

FIGURE 3 Processing of electron micrographs. A single field is shown after the following stages of image processing for a 1.5% underivatized agarose gel: (*a*) digitization, (*b*) reduction of noise and sharpening of edges, (*c*) thresholding and binarization, and (*d*) skeletonization. The length of the bar is 2000 nm.

to one pixel wide lines (Fig. 3 *d*). The values of L_V and M_L are in Table 1 for each value of A used.

From binary images constructed by use of the procedure of Fig. 3 (i.e., Fig. 3*c*), the fraction (F) of chords that had a length, $2P_c$, was determined as a function of P_c. During determination of F versus P_c, the chords were produced by passing neighboring parallel lines through an entire randomly-oriented image. If the gel is isotropic, this procedure is equivalent to using randomly-oriented lines (33, 37). The P_c values were obtained in pixels (i.e., all values are members of a discrete set) at a magnification of 10 nm per pixel. Five independent images of randomly chosen fields (36 μm^2) were used. The result for the 0.4% gel of Fig. 1 was a semilogarithmic F versus P_c plot that could be represented by two straight lines (Fig. 4 *a*). The line for the lower P_c values (first phase) had a slope (k_1) that was 3.9 × the slope (k_2) of the line for the higher P_c values (second phase). Because of sampling error, the deviation from the fitted line increased as P_c increased.

When A was raised to 1.0 and 1.5, the magnitude of k_2 increased, without significant change in k_1; the plot became monophasic for 1.5% agarose (Fig. 4 *b*; the A value is indicated in the figure). When A was further raised to 2.5 (Fig. 4 *b*), the magnitude of both k_1 and k_2 increased; k_1 became 0.85 × k_2, thereby reversing the curvature of the semilogarithmic F versus P_c plot (all values of k_1 and k_2 are in Table 1).

Of the procedures used for image processing, thresholding has the greatest potential for introducing error. Thus, the analysis of Fig. 4 was repeated by use of thresholds that were at either the upper or lower limits consistent with the criterion for thresholding described above. For a 1.5% gel, these changes resulted in mean P_c values changed by ±6%.

Comparison of the observed P_c distribution with that of a random fiber gel

To understand the relationship of agarose gels to random fiber gels, the F versus P_c relationship was also determined for computer-simulated (see the Materials and Methods section) projections of sections of random fiber gels. In so doing, a value must be chosen for both the thickness of the projected section and the dimensions of fibers in the random fiber gel. However, whatever the thickness of sections, the anticipation is that the F versus P_c relationship will be a Poisson distribution. The reasons for this proposal are the following: (*a*) For an infinitely thin section, the gel approximates a random array of circular elements; a Poisson distribution has already been demonstrated in this case (33). (*b*) For a section that has a thickness much greater than the length of a fiber, empirical analysis of a random fiber gel also yields a Poisson distribution (procedures are described in the next paragraph). A Poisson distribution is equivalent to a linear plot of log F versus P_c in Fig. 4. Thus, as found for a 1.5% agarose gel in

TABLE 1 Analysis of electron micrographs*

A (%)	$-k_1$(nm^{-1}) × 10^{-3}	$-k_2$(nm^{-1}) × 10^{-3}	$\bar{P}_c$(nm) × 10^2±10%	σ(nm) × 10^2±10%	$\hat{P}_c$(nm) × 10^2±10%	L_V(nm^{-2}) × 10^{-5}±10%	M_L(ng/nm) × 10^{-10}¶
Underivatized							
0.4	4.70	1.20	3.0	3.3	3.2	2.1	1.9
0.6	3.32	1.62	2.4	2.5	2.5	2.7	2.2
0.8	4.10	1.98	2.2	2.2	2.2	3.5	2.3
1.0	3.53	2.60	1.8	1.8	1.8	3.7	2.7
1.2	3.90	2.88	1.4	1.5	1.5	4.2	2.9
1.5	5.82	5.80	1.2	1.2	1.2	7.4	2.0
2.0	6.44	6.82	0.75	0.68	0.71	8.1	2.5
2.5	7.18	8.48	0.68	0.62	0.68	9.5	2.6
Derivatized							
0.4	4.56	2.32	1.9	2.1	2.0	3.6	1.1
0.6	4.72	3.64	1.2	1.3	1.3	4.7	1.3
0.8	4.64	3.74	1.1	1.2	1.2	5.4	1.5
1.0	5.72	4.18	0.90	0.91	0.91	6.4	1.6
1.2	6.36	4.62	0.84	0.86	0.85	6.5	1.8
1.5	8.00	7.86	0.60	0.55	0.57	9.6	1.6
2.0	9.18	12.0	0.54	0.47	0.50	10.2	2.0
2.5	10.9	10.6	0.48	0.41	0.45	10.2	2.5
Random fiber							
‡	§						
0.4	1.68		3.7	3.7	3.7		
0.6	2.40		2.6	2.5	2.5		
0.8	3.65		2.0	2.0	2.0		
1.0	3.76		1.6	1.6	1.6		
1.2	4.42		1.4	1.3	1.4		
1.5	5.24		1.1	1.1	1.1		
2.0	6.95		0.84	0.81	0.83		
2.5	9.28		0.69	0.65	0.67		

* Quantities were determined from histograms by procedures described in the text.

‡ Equivalent gel concentration.

§ Only k_1 was observed.

¶ The mass per length of an agarose double helix is 1.71 × 10^{-12} ng/nm (10).

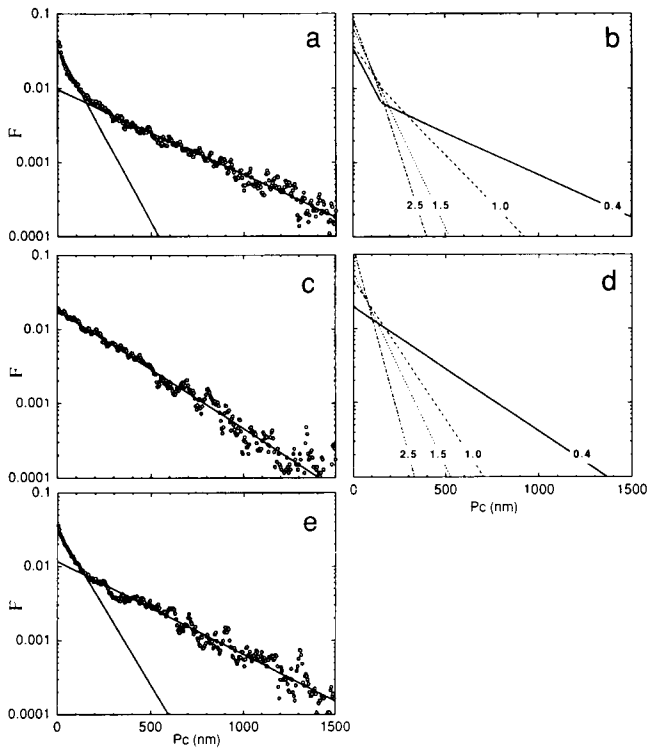

FIGURE 4 Semilogarithmic F versus P_c plots. Semilogarithmic F versus P_c plots are shown for: (a) an underivatized 0.4% agarose gel; all points are shown, together with a biphasic, best-fit line, (b) several underivatized agarose gels; the A is indicated in the figure; points are not shown, (c) a computer-simulated projection of an 0.4% random fiber gel; all points are shown, together with a monophasic, best-fit line, (d) several computer-simulated projections of random fiber gels; the effective gel percentage is indicated in the figure; points are not shown, (e) a computer-simulated projection of a gel that has randomly oriented fibers connected in pairs at their centers; the pairs of fibers were randomly placed; all points are shown.

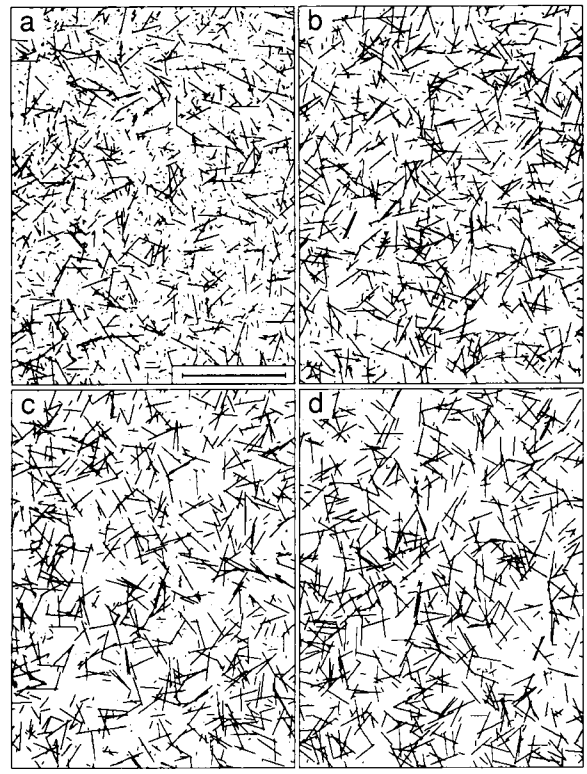

FIGURE 5 Projections of a section of a random fiber gel as a function of the thickness of the section. The following ratios of section thickness to fiber length (500 nm) were used: 0.2 (a), 0.5 (b), 1.0 (c), 2.0 (d). The length of the bar is 2000 nm.

Fig. 4 b, the proposal is that log F versus P_c plots will be linear for random fiber gels.

To further test this proposal, computer-simulated projections of sections of random fiber gels were constructed by use of fibers that had the length of the longest uninterrupted fibers of a 1.5% gel, 500 nm; the fiber width was 20 nm. Projections were made for several values of section thickness by use of a total fiber length per area that was equal to that of the electron micrograph of a 1.5% gel. As expected, the percentage of fibers seen in cross section decreased as the section thickness/fiber length ratio increased from 0.2 (Fig. 5 a) to 0.5 (Fig. 5 b), 1.0 (Fig. 5 c), and 2.0 (Fig. 5 d). When compared to sections of agarose gels in Figs. 1 and 2, the random fiber gel is most realistic in either Fig. 5, b or c. A linear log F versus P_c plot was observed not only for the gels of Fig. 5, b and c, but also for those in Fig. 5, a and d; for the gel in Fig. 5 c, the plot is shown in Fig. 4 d. Linearity was maintained when the fiber thickness was either increased or decreased by a factor of 2 (not shown). Thus, the above proposal is correct.

After analyzing the computer-generated, random fiber equivalent of a 1.5% gel, the random fiber equivalents of other gels were generated by changing the total fiber length per area, in proportion to A. Random fiber gels were projected (section thickness as in Fig. 5 c) with fiber concentrations equivalent to those of agarose gels with A values of 0.4% (Fig. 6 a), 1.0% (Fig. 6 b) and 2.5% (Fig. 6 d). The semilogarithmic F versus P_c relationship (shown together with data in Fig. 4c for $A = 0.4$) for the 0.4, 1.0, and 2.5% random fiber gels was linear, i.e., monophasic (Fig. 4d). When compared to agarose gels (Fig. 4b; Table 1), the most striking difference was observed for the 0.4% gel (see also, k_1 and k_2 in Table 1).

Values of both P_E and the averaged P_c as a function of A

To determine the relationship of gel structure to the sieving observed during electrophoresis through an underivatized agarose gel, (a) both the root mean square value of P_c ($\hat{P}_c$) and the mean value of P_c ($\bar{P}_c$) were determined as a function of A, and (b) these averaged P_c values were compared to P_E. For computer-simulated projections of random fiber gels (constructed by the procedure of Fig. 6), a log-log plot of $\hat{P}_c$ versus A was linear for $0.4 \leq A \leq 2.5$ (Fig. 7 a). However, the point for $A = 0.2$ in Fig. 7a fell below the straight line that fit the data at higher A values. In the region of linearity: (a) this plot had a slope (x) equal to –0.93, and (b) the same plot for $\bar{P}_c$ was also linear when $A \geq 0.4$; the slope was –0.93 (Table 2). The loss of linearity at $A = 0.2$ appears to be caused

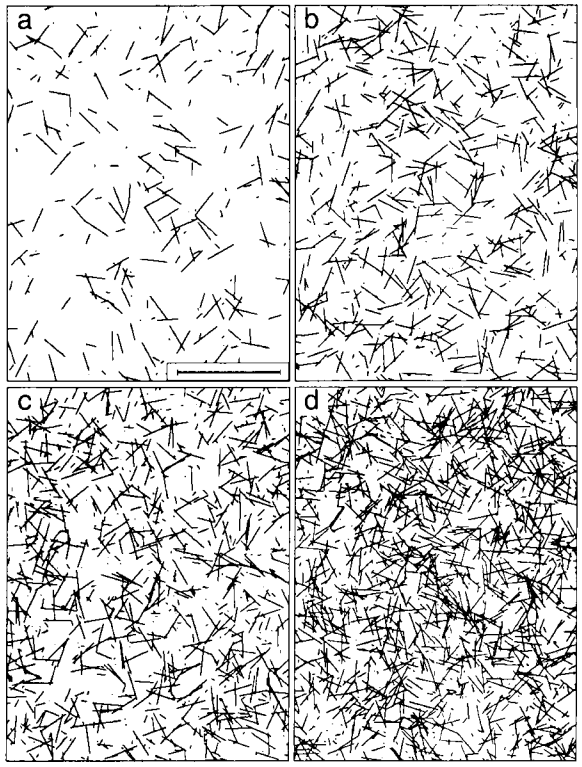

FIGURE 6 Random fiber gels as a function of A. Generation of gels was performed by procedures described under Materials and Methods. The section thickness was 1.0 × the fiber length. The effective gel percentage was: 0.4 (*a*), 1.0 (*b*), 1.5 (*c*), 2.5 (*d*). The length of the bar is 2000 nm.

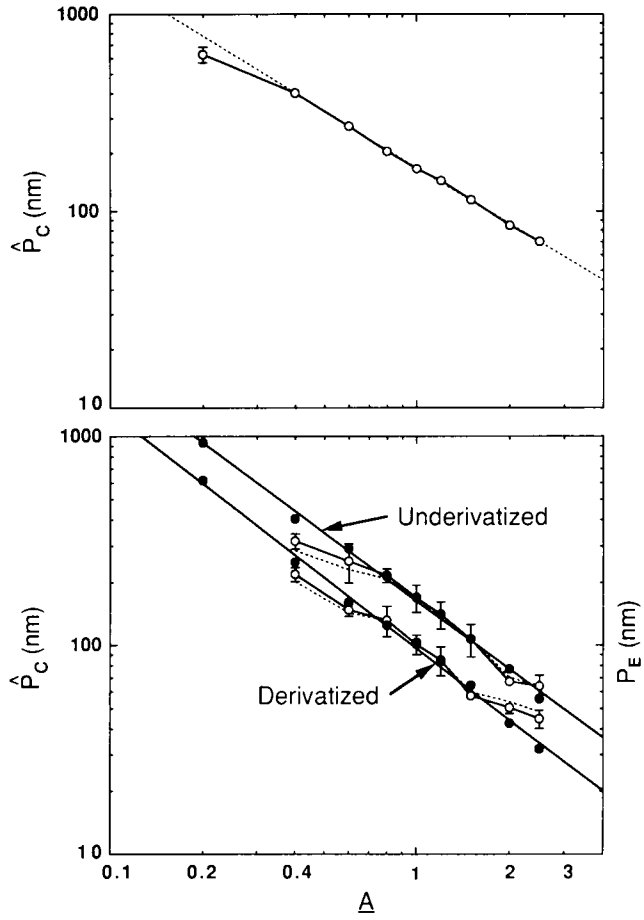

FIGURE 7 $\bar{P}_c$, $\hat{P}_c$, and P_E as a function of A. (*a*) $\hat{P}_c$ for computer-generated, random-fiber gels (Fig. 6) as a function of the effective gel percentage, (*b*) $\hat{P}_c$ (*empty symbols*), and P_E (*filled symbols*) for both derivatized and underivatized agarose gels as a function of A; $\bar{P}_c$ versus A is plotted as a dashed line. In (*a*), the error for A values greater than 0.2 is smaller than the radius of a data point.

by the following aspect of the data processing. As the gels became more dilute, an increasing fraction of initiated chords were not terminated, because the scan left the electron micrograph; this loss occurred preferentially for chords with the higher P_c values. When the thickness of the fibers was either doubled or halved in the random fiber gel, the value of x was unchanged. Thus, within the experimental error for agarose gels, fiber thickness does not have a detectable effect on x.

When made from data obtained from an underivatized agarose gel, a log-log plot of $\hat{P}_c$ versus A was, like the plot for a random fiber gel, linear for $A \geq 0.8$ (*empty symbols* and *solid line* in Fig. 7b, underivatized). However, the points for $A = 0.4$ and 0.6 appeared to fall below the straight line that fit the data for higher A values. Because this observation has been repeated in a second experiment for which a different lot of underivatized, Seakem LE agarose was used (data not shown), it will be assumed to be significant. In the region of linearity, the slope of this plot was −1.1. When $\bar{P}_c$ was plotted instead of $\hat{P}_c$, the plot was only slightly altered (dashed line without symbols in Fig. 7b, underivatized).

To compare $\hat{P}_c$ to P_E for underivatized agarose, a log-log plot of the (sieving-based) P_E versus A relationship (filled symbols in Fig. 7b, underivatized) was superimposed on the (electron microscopy-based) $\hat{P}_c$ versus A plot (empty symbols in Fig. 7b, underivatized). The vertical $\hat{P}_c$ axis was (arbitrarily) scaled to make the plots equal for $A = 1$. After curve fitting, the values of both P_E at $A = 1$ ($P_E(1)$) and $\hat{P}_c$ at $A = 1$ ($\hat{P}_c(1)$) are in Table 2. Like the $\hat{P}_c$ versus A plot for $A \geq 0.8$, the P_E versus A plot was linear; the slope for the P_E versus A plot was −1.1, not significantly different from the slope of the linear segment of the $\hat{P}_c$ versus A plot. Linearity for the P_E versus A plot extended to $A = 0.2$, beyond the point at which the $\hat{P}_c$ versus A plot became nonlinear. Thus, for $A \geq 0.8$, P_E can be determined from either $\hat{P}_c$ or $\bar{P}_c$ by multiplying by a constant. In Fig. 5b, this constant was 1.5 for $\hat{P}_c$ and 1.1 for $\bar{P}_c$. This linear relationship of P_E to $\hat{P}_c$ leads to the following question. When (*a*) thin sections used to determine $\hat{P}_c$ have invariant thickness and (*b*) log-log $\hat{P}_c$ versus A plots are linear, is the $P_E/\hat{P}_c$ ratio a constant independent of other characteristics of gels?

Comparison with derivatized agarose

To help answer this question, the analysis of Fig. 7 was performed for a derivatized (hydroxypropyl) agarose that produced P_E values lower than those of underivatized agarose at a given A value (Table 2). Unlike other preparations of agarose that have comparatively small P_E values (16) the

TABLE 2 Relationship of averaged gel structure to sieving*

Gel type	$P_E(1)$ (nm) ± 5	$-x$ ± 0.1	$\bar{P}_c(1)$ (nm) ± 10	$-x$ ± 0.1	$\hat{P}_c(1)$ (nm) ± 10	$-x$ ± 0.1
Underivatized	162	1.1	164	1.1	168	1.1
Derivatized	96	1.1	100	0.90	100	0.98
Random			162	0.93	160	0.93

* Quantities were determined by curve fitting the data for the range $0.8 \leq A \leq 2.5$ according to the equation $P(A) = P(1)A^{-x}$. Each x belongs with the type of pore size measurement to its left.

hydroxypropyl agarose could be thin-sectioned (without breakage during embedding) at concentrations as low as 0.4%. When both the $\hat{P}_c$ versus A and P_E versus A relationships were examined for the derivatized agarose (Fig. 7b, derivatized), the following observations were made: (*a*) For $0.8 \leq A \leq 2.0$, the $\hat{P}_c$ and P_E were reduced by the same factor, within experimental error; the scale of $\hat{P}_c$ for the derivatized agarose is that of the underivatized agarose in Fig. 7b. (*b*) A loss of linearity occurred at the lower A values, 0.4 and 0.6; significant nonlinearity occurred at $A = 2.5$. Thus, for both $0.8 \leq A \leq 2.0$, and the two most differing gel preparations that could be analyzed, $P_E/\hat{P}_c$ was a constant, independent of both A and the P_E versus A relationship. For A values below this range, the variation of $P_E/\hat{P}_c$ is further discussed in the next section. As found for underivatized agarose, only slight changes were observed when $\bar{P}_c$ was used instead of $\hat{P}_c$ (*dashed line* in Fig. 7b, derivatized).

At the level of the semilogarithmic F versus P_c plot for the derivatized agarose, the primary reason for the reduction in $\hat{P}_c$ values was that k_2 was higher for the derivatized agarose than it was for the underivatized agarose. However, at the higher A values, k_1 was also significantly higher for the derivatized agarose (Table 1). As was the case for underivatized agarose, k_1 values initially were comparatively constant and subsequently increased, as the value of A increased (Table 1).

DISCUSSION

Preservation of structure in the images presented here depends on (*a*) absence of movement of fibers during both dehydration and other steps in preparation for thin sectioning, (*b*) uniformity in the staining of agarose, and (*c*) visualization of all fibers, independent of either radius or orientation. Based on the absence of detectable alteration in the size of agarose gels during embedding (Refs. 9 and 10 and Materials and Methods), the assumption is made here that the network of agarose does not either expand or contract during preparation of thin sections for electron microscopy. Therefore, the agarose fibers are assumed not to have moved. The extent to which staining was uniform is not known. However, modeling revealed that both the shape of F versus P_c plots and the slope of $\hat{P}_c$ versus A plots were independent of the radius of fibers for a four-fold range of radii. Thus, nonuniformity of staining is not considered significant in the interpretations presented here. The fraction of fibers imaged is also not known. As fibers became thinner, this fraction might have become significantly lower than one. The thinner fibers most orthogonal to the plane of the section would be the fibers most likely to be lost in the background grain. The following qualitative observation made here is explained by the assumption that the fraction of fibers imaged decreased as the fibers became more orthogonal to the plane of the section: To obtain the best visual match between a computer-generated random fiber gel projection and an electron micrograph, the section thickness/fiber length ratio for the random fiber gel projection was 2–4-fold higher than the estimate of this ratio for an electron micrograph of a comparable agarose gel. Assuming that the fraction of agarose fibers imaged did not vary with either location in a thin section or concentration (or type) of agarose, the conclusions drawn below are not influenced by the fraction of fibers imaged. These conclusions are based on comparison of different values of either P_c or $\hat{P}_c$, all obtained by the same procedure. However, any conclusions based on noncomparative use of either P_c, $\hat{P}_c$, or $P_E/\hat{P}_c$ would be influenced by the fraction of fibers imaged.

For a 1.5% underivatized agarose gel, the linearity of the semilogarithmic F versus $\hat{P}_c$ plot of Fig. 4 *b* indicates that this network has a Poisson distribution of $\hat{P}_c$ values (33). This conclusion is confirmed by the equality of $\bar{P}_c$ and the standard deviation (σ) of P_c for a 1.5% underivatized agarose gel (Table 1). A Poisson distribution was also found in Fig. 4d for the computer-generated 1.5% random fiber gel of Fig. 6c (Fig. 4d; Table 1). Thus, the 1.5% gel of underivatized agarose was indistinguishable from a random fiber gel.

Analytical description of random fiber gels has previously been performed by use of a pore radius defined to be the radius of the largest randomly placed sphere that doesn't intersect a fiber of gel. This definition, different from the definition used here, yields a radius of the effective pore that varies as the 0.5 power of A (i.e., $x = -0.5$, (38)). The use of $\hat{P}_c$, as defined in the alternative description of the present study, yields an x for a random fiber gel (−0.93) that more closely approximates the x of either $\hat{P}_c$ or P_E measured for the agarose preparations characterized in the present study (Table 2). A possible explanation for this observation is that (*a*) sieving during gel electrophoresis is determined by non-equilibrium movement of particles; therefore, sieving would not (as an equilibrium process such as partitioning would) be a simple function of excluded volume in three dimensions, and (*b*) instead, sieving is a function of either area excluded in planes of entry or the hydrodynamics of movement in spaces formed by the gel; values of P_E are compatible with either of these latter two possibilities (16). The value of x was not a constant among different preparations of agarose, even among preparations that had the same electroosmosis. For

the range of A values used here, preparations of Seakem LE agarose have had values of x that varied significantly from −0.84 to −1.1, when measured for P_E by use of the procedures used for Fig. 7. Values of $P_E(1)$ varied from 147 to 164; this latter difference is not significant (data not shown). Thus, for accuracy, the sieving of a gel must always be compared to the structure of the same preparation of gel.

As A either increased or decreased from 1.5, the data of Table 1 indicate that the change from a monophasic (random fiber) to a biphasic (nonrandom fiber) F versus P_c plot was caused by a k_2 that was more sensitive to A than k_1. In agreement, the light scattering from agarose gels has previously been qualitatively interpreted by the assumption that agarose gel fibers become less randomly arranged as A decreases from 1.5 (39). A possible explanation is that the smaller pores (i.e., those that yield k_1) were formed by neighboring fibers (each fiber a lateral aggregate of narrower fibers) that were at junction zones at which fibers branch (for a theoretical discussion, see Ref. 40). An electron micrograph of a negatively stained, branched agarose fiber has previously been presented (2). By this hypothesis, as A either decreased or increased from 1.5, the agarose fiber concentration in junction zones remained comparatively unaltered, while the agarose fiber concentration in interjunction zone regions varied more rapidly as a function of A. To test this hypothesis, computer-simulated projections were produced after altering the procedure used for Fig. 6 in the following way: Instead of using single, linear fibers as the units for random placement, branched aggregates consisting of two randomly oriented fibers joined at their centers were used as the units for random placement. The result was the production of simulated two-dimensional gel projections that yielded a biphasic semilogarithmic F versus P_c plot for a 0.4% gel (Fig. 4 *e*). Qualitatively, these plots had the changes in k_1 and k_2 that were observed for agarose gels in Fig. 4 (data not shown). Thus, the data are possibly explained by the hypothesis that branches are the primary source of perturbation in the random fiber character of the underivatized agarose gels. An alternative possible explanation of this perturbation is pre-gelation inhomogeneity of the agarose solution. Pre-gelation inhomogeneity has been demonstrated for underivatized agarose solutions gelled at temperatures higher than those used here (41–43). At the temperature used here to gel agarose, this inhomogeneity either doesn't occur or occurs too rapidly for detection. Thus, the occurrence of junction zones is the more plausible explanation. These conclusions are based on statistics. That is, they are not based on criteria for identifying an isolated junction zone.

To ultimately develop a physical theory that describes the sieving of spheres by gels, the relationship of structure to sieving must be determined. The invariant $P_E/\hat{P}_c$ ratio for $0.8 \leq A \leq 2.0$ indicates that the concept of microscopic pore radius is related to the construct (P_E) used to describe the (macroscopically observed) sieving of agarose gels. This observation is a constraint on detailed theories that describe the resistance to motion in fibrous networks.

Linear correlation of $\hat{P}_c$ and P_E was lost at the lower A values because of a decrease in the magnitude of the slope of the log-log $\hat{P}_c$ versus A plot, but not the log-log P_E versus A plot. At least three explanations for this phenomenon are possible: 1) Sampling errors occurred during determination of $\hat{P}_c$ at the lower A values. 2) At the lower A values, some of the fibers observed in thin sections were not effective in sieving. 3) At the lower A values, the nonrandom fiber character of the gel disrupted the linearity of the $\hat{P}_c$ versus A relationship. Although sampling error did not occur for the 0.4–2.5% random fiber gels, it did appear to occur for the 0.2% random fiber gel. Thus, possibly, explanations 1 and 3 both contribute. That is, the nonrandom fiber character of the gel increases the A value at which sampling errors begin. However, explanation 2 is also plausible. Candidates for the nonsieving fibers in explanation 2 are the projecting (dead-end) agarose fibers that increase in number as A decreases, when observed in freeze-dried gels (12). These fibers are also possibly the cause of the atypical sieving observed in 0.2–1.0% agarose, for open circular DNA (reviewed in Ref. 2). Evaluating these explanations should be assisted by quantitative analysis of both the sieving and structure of gels that have P_c values more variable than the P_c values of the gels investigated here.

We thank E. Anthony Meyer and Debbie Lackan for technical assistance, Shirley J. Hayes for providing bacteriophages T3 and ϕII, Margaret M. Miller, Dena M. Edwards-Stark and Christina Odom for performing electron microscopy, and Linda C. Winchester for typing this manuscript.
Support was received from the National Science Foundation (grant DMB 9003695) and the Robert A. Welch Foundation (grant AQ-764).

REFERENCES

1. Sambrook, J., E. F. Fritsch, and T. Maniatis. 1989. Molecular Cloning: A Laboratory Manual, Chap. 13, Cold Spring Harbor Laboratory Press, Cold Spring Harbor, NY.
2. Serwer, P. 1990. Sieving by agarose gels and its use during pulsed field electrophoresis. *Biotech. Genet. Eng. Rev.* 8:319–343.
3. Cantor, C. R., C. L. Smith, and M. K. Mathew. 1988. Pulsed field gel electrophoresis of very large DNA molecules. *Ann. Rev. Biophys. Biophys. Chem.* 17:287–304.
4. Nordén, B., C. Elvingson, M. Jonsson, and B. Åkerman. 1991. Microscopic behavior of DNA during electrophoresis: electrophoretic orientation. *Quart. Rev. Biophys.* 24:103–164.
5. Viovy, J. L. and A. D. Défontaines. 1992. Reptation theory of pulsed electrophoresis and trapping electrophoresis. *In* Pulsed-Field Gel Electrophoresis: Protocols, Methods and Theories. M. Burmeister and L. Ulanovsky, editors. Humana Press, Totowa, NJ. 403–450.
6. Zimm, B. H. and S. D. Levene. 1992. Problems and prospects in the theory of gel electrophoresis of DNA. *Quart. Rev. Biophys.* 25:171–204.
7. Calladine, C. R., C. M. Collis, H. R. Drew, and M. R. Mott. 1991. A study of electrophoretic mobility of DNA in agarose and polyacrylamide gels. *J. Mol. Biol.* 221:981–1005.
8. Madden, T. L. and J. M. Deutsch. 1991. Theoretical study of DNA during orthogonal field alternating gel electrophoresis. *J. Chem. Phys.* 94:1584–1591.
9. Amsterdam, A., Z. Er-el, and S. Shaltiel. 1975. Ultrastructure of beaded agarose. *Arch. Biochem. Biophys.* 171:673–677.
10. Attwood, T. K., B. J. Nelmes, and D. B. Sellen. 1988. Electron microscopy of beaded agarose gels. *Biopolymers.* 27:201–212.
11. Waki, S., J. D. Harvey, and A. R. Bellamy. 1982. Study of agarose gels by electron microscopy of freeze-fractured surfaces. *Biopolymers.* 21: 1909–1926.

12. Whytock, S. and J. Finch. 1991. The substructure of agarose gels as prepared for electrophoresis. *Biopolymers.* 31:1025–1028.
13. Dea, I. C. M., A. A. McKinnon, and D. A. Rees. 1972. Tertiary and quaternary structure in aqueous polysaccharide systems which model cell wall cohesion: reversible changes in conformation and association of agarose, carrageenan and galactomannans. *J. Mol. Biol.* 68:153–172.
14. Norton, I. T., D. M. Goodall, K. R. J. Austen, and E. R. Morris. 1986. Dynamics of molecular organization in agarose sulphate. *Biopolymers.* 25:1009–1029.
15. Griess, G. A. and P. Serwer. 1989. Structure of agarose gels: mean pore radius. *Proc. Electron Microscopy Soc. Am.* 47:884–885.
16. Griess, G. A., E. T. Moreno, R. A. Easom, and P. Serwer. 1989. The sieving of spheres during agarose gel electrophoresis: quantitation and modeling. *Biopolymers.* 28:1475–1484.
17. Serwer, P. 1986. Use of gel electrophoresis to characterize multimolecular aggregates. *Methods Enzymol.* 130:116–132.
18. Kirkpatrick, F. H., K. Guiseley, R. Provonchee, and S. Nochumson. 1991. High gel strength low electroendosmosis agarose. U. S. Patent 4,983,268.
19. Guiseley, K. 1976. Modified agarose and agar and method of making same. U. S. Patent 3,956,273.
20. Serwer, P., R. H. Watson, S. J. Hayes, and J. L. Allen. 1983. Comparison of the physical properties and assembly pathways of the related bacteriophages T7, T3 and ϕII. *J. Mol. Biol.* 170:447–469.
21. Serwer, P. and F. J. Dunn. 1990. Rotating gels: Why, how and what. *Methods: A Companion to Methods Enzymol.* 1:143–150.
22. O'Neill, R. R., L. G. Mitchell, C. R. Merrill, and W. S. Rasband. 1989. Use of image analysis to quantitate changes in form of mitochondrial DNA after x-irradiation. *Appl. Theor. Electrophor.* 1:163–167.
23. Glauert, A. M. 1978. Practical Methods in Electron Microscopy: Fixation, Dehydration and Embedding of Biological Specimens, North Holland Publishing Company, Amsterdam.
24. Peachy, L. D. 1958. Thin sections: I. A study of section thickness and physical distortion produced during microtomy. *J. Biophys. Biochem. Cytol.* 4:233–242.
25. Zelander, T. and R. Ekholm. 1960. Determination of the thickness of electron microscopy sections. *J. Ultrastruct. Res.* 4:413–419.
26. Hayat, M. A. 1970. Principles and Techniques of Electron Microscopy: Biological Applications, Vol. 1, Van Nostrand Reinhold Co., New York.
27. Estrada, J. C., N. T. Brinn, and E. H. Bossen. 1985. A rapid method of staining ultrathin sections for surgical pathology TEM with the use of the microwave oven. *Am. J. Clin. Pathol.* 83:639–641.
28. Reynolds, E. S. 1963. The use of lead citrate at high pH as an electron-opaque stain in electron microscopy. *J. Cell Biol.* 17:208–212.
29. Griess, G. A., E. T. Moreno, and P. Serwer. 1992. Desktop, digital imaging: application to detection of length heterogeneity after hyperresonant pulsed-field gel electrophoresis of mature bacteriophage P22 DNA. *In* Pulsed Field Gel Electrophoresis, M. Burmeister and L. Ulanovsky, editors. Humana Press, Totowa, New Jersey, 173–181.
30. Arnott, S., A. Fulmer, W. E. Scott, I. C. M. Dea, R. Moorhouse, and D. A. Rees. 1974. The agarose double helix and its function in agarose gel structure. *J. Mol. Biol.* 90:269–284.
31. Foord, S. A. and E. D. T. Atkins. 1989. New x-ray diffraction results from agarose: extended single helix structures and implications for gelation mechanism. *Biopolymers.* 28:1345–1365.
32. Attwood, T. K. and D. B. Sellen. 1990. An x-ray diffraction study of agarose gel as a function of concentration. *Biopolymers.* 29:1325–1328.
33. Russ, J. C. 1990. Computer-Assisted Microscopy: The Measurement and Analysis of Images. Plenum Press, New York.
34. Marr, D. and E. Hildreth. 1980. Theory of edge detection. *Proc. R. Soc. London Serial B.* 207:187–217.
35. Smith, T. G., Jr., W. B. Marks, G. D. Lange, W. H. Sheriff, Jr., and E. A. Neale. 1988. Edge detection in images using Marr-Hildreth filtering techniques. *J. Neurosci. Methods.* 26:75–82.
36. Dudgeon, D. E. and R. M. Mersereau. 1984. Multidimensional Digital Signal Processing, Prentice-Hall, Englewood Cliffs, NJ.
37. Underwood, E. E. 1970. Quantitative Stereology, Addison Wesley, Reading, MA.
38. Ogston, A. G. 1958. The spaces in a uniform random suspension of fibres. *Trans. Faraday Soc.* 54:1754–1757.
39. Key, P. Y. and D. B. Sellen. 1982. A laser light-scattering study of the structure of agarose gels. *J. Polymer Sci.: Polymer Phys. Ed.* 20:659–679.
40. West, R. 1987. The distribution of void sizes in a reticulate gel. *Biopolymers.* 26:343–350.
41. San Biagio, P. L., F. Madonia, J. Newman, and M. U. Palma. 1986. Sol-sol structural transition of aqueous agarose systems. *Biopolymers.* 25:2255–2269.
42. Leone, M., F. Sciortino, M. Migliore, S. L. Fornili, and M. B. P. Vittorelli. 1987. Order parameters of gels and gelation kinetics of aqueous, agarose systems: relation to the spinodal decomposition of the sol. *Biopolymers.* 26:743–761.
43. Emanuele, A., L. Di Stefano, D. Giacomazza, M. Trapanese, M. B. Palma-Vittorelli, and M. U. Palma. 1991. Time-resolved study of network self-organization from a biopolymeric solution. *Biopolymers.* 31: 859–868.